JCTC Journal of Chemical Theory and Computation

Article

pubs.acs.org/JCTC

Materials Design On-the-Fly

Tiago F. T. Cerqueira,[†,‡] Rafael Sarmiento-Pérez,[‡,†] Maximilian Amsler,[§] F. Nogueira,[∥] Silvana Botti,[†,‡] and Miguel A. L. Marques*[,#,‡]

[†]Institut für Festkörpertheorie und -optik, Friedrich-Schiller-Universität Jena and European Theoretical Spectroscopy Facility, Max-Wien-Platz 1, 07743 Jena, Germany

[‡]Institut Lumière Matière, UMR5306 Université Lyon 1-CNRS, Université de Lyon, F-69622 Cedex Villeurbanne, France

[§]Department of Physics, Universität Basel, Klingelbergstrasse 82, 4056 Basel, Switzerland

[∥]Centro de Física Computacional, Departamento de Física, Universidade de Coimbra, Rua Larga, 3004-516 Coimbra, Portugal

[#]Institut für Physik, Martin-Luther-Universität Halle-Wittenberg, D-06099 Halle, Germany

ABSTRACT: The dream of any solid-state theorist is to be able to predict new materials with tailored properties from scratch, i.e., without any input from experiment. Over the past decades, we have steadily approached this goal. Recent developments in the field of high-throughput calculations focused on finding the best material for specific applications. However, a key input for these techniques still had to be obtained experimentally, namely, the crystal structure of the materials. Here, we give a step further and show that one can indeed optimize material properties using as a single starting point the knowledge of the periodic table and the fundamental laws of quantum mechanics. This is done by combining state-of-the-art methods of global structure prediction that allow us to obtain the ground-state crystal structure of arbitrary materials, with an evolutionary algorithm that optimizes the chemical composition for the desired property. As a first showcase demonstration of our method, we perform an unbiased search for superhard materials and for transparent conductors. We stress that our method is completely general and can be used to optimize any property (or combination of properties) that can be calculated in a computer.

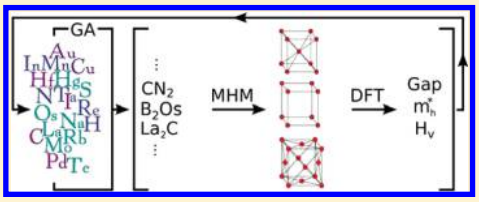

1. INTRODUCTION

One of the most exciting developments in condensed matter over the past years is, without doubt, materials design.[1−4] This new discipline aims at solving the so-called inverse problem: given a certain desired property (or properties), discover (design) the material that possesses this property under a given set of constraints. These constraints can be related to the mechanical or chemical stability of the compounds, their price, their availability, etc. Several groups are actively working on this topic, with many projects related to energy materials including lithium batteries,[3] photovoltaics,[5,6] and so on.

A typical materials design project starts with the creation of a database that contains calculations for a large selection of experimentally known systems. For crystalline inorganic solids the largest experimental database available to date is the Inorganic Crystal Structure Database[7] (ICSD), containing more than 170,000 structures. These are then filtered, eliminating duplicates, alloys, or insufficiently characterized structures (such as the ones lacking the positions of hydrogens). The remaining (currently around 50,000) are then calculated systematically and stored in a database.[8,9] These structures are often complemented by theoretical compounds obtained by chemical substitution in known crystal structures.[10,11] All of these calculations are performed with some flavor of density functional theory.[12,13] This choice is well motivated by the fact that density functional theory is by now the only theory that is able to provide a convenient accuracy for a relatively moderate computational effort.

These databases of ab initio results can then be filtered to yield the best material according to some objective function[14,15] or used as a training set for some machine learning algorithm that will extrapolate the information to obtain new crystal structures with improved properties.[16,17]

Even if this framework is extremely powerful and has led to a number of significant discoveries, in our opinion it suffers from a few drawbacks. First of all, it requires an enormous amount of experimental input, and in fact at least 50,000 complex synthesis and X-ray diffraction experiments had to be realized in order to obtain the current databases. Although 50,000 may seem like a large number, it is certainly a small fraction of the number of all possible (thermodynamically) stable compounds. Of course each new experimental entry that is added to the database encompasses substantial costs in personnel, equipment, and consumables. Second, any prediction based on this set will be biased by the subset of systems studied experimentally. If the solution for a given materials design problem lies in a region that has been unpopular among chemists and crystallographers, it is very unlikely that it will ever be found by any algorithm. Third, experimentally we know mostly stable stoichiometries. This means that large regions of (the unstable) phase space are completely unrepresented in the databases, which makes bridging these regions during an optimization procedure extremely difficult.

Received: March 4, 2015
Published: June 30, 2015

DOI: 10.1021/acs.jctc.5b00212
J. Chem. Theory Comput. 2015, 11, 3955−3960

Finally, the dream of any theoretician is to be able to provide predictions with as little experimental information as possible (ideally none). In the following we will show that this is to some extent possible and that one can nowadays perform the inverse problem in an efficient way without resorting to databases or to any experimental input besides the periodic table of the elements and the laws of quantum mechanics.

There are other approaches to the design of new materials that do not require databases. For example, the concept of energy gradients in chemical compound space[18−23] (the so-called alchemical derivatives), transforming the discrete optimization problem into a continuum one, has been proposed as a way to optimize molecular properties. Evolutionary approaches have also been used, although always with rather severe constraints. For example, refs 5 and 6 optimized optical absorption by changing the ratio and the order of Si and Ge monolayers, while in ref 24 the ground state for $Au_{1-x}Pd_x$ (with variable x) alloys was found but for a fixed Bravais lattice. On the other hand, variable composition genetic algorithms were proposed to study binary phase diagrams, with applications, e.g., to the Mn−B system.[25]

Our approach tries to overcome several limitations of the previous techniques and is composed of three parts. In the first, we use a multiobjective genetic algorithm (GA) to vary the composition of the unit cell in order to maximize a set of properties. Then, for each individual (i.e., for each composition that stemmed from the GA) we use a global structural prediction method[26] to obtain its ground-state crystal structure. Finally, the property (or properties) that we want to optimize is (are) calculated for the ground state and possibly for the lowest lying metastable structures. These are finally fed back into the GA in order to determine the better fit parents that will generate the offspring for the following generation.

2. METHODS

We analyze in more detail the single steps that compose our calculations. To perform the multiobjective optimization, we used the nondominated sorting genetic algorithm−II.[27] The gene describing each individual was given by a sequence of six integer numbers, each one indicating a different chemical element. In order to accommodate unit cells with less atoms, we introduced an empty "atom". The ordering of the sequences was taken into account, such that, e.g., ABC is equivalent to BCA. The mating operator simply mixed the chemical composition of both parents, while mutations transmuted randomly one element in the gene. The mutation rate was set to 10%. In our current implementation we did not make use of a Lamarckian-type evolution as described in ref 24. However, we expect that such ideas could be applied to obtain a speed up of the convergence of our method.

The key ingredient that allows us to perform the inverse problem on-the-fly, without the use of any precomputed database, is the minima hopping method for global structural prediction.[28,29] This is an efficient crystal-structure prediction algorithm designed to determine the low-energy structures of a system given solely its chemical composition. At a given chemical composition and at a given pressure, the enthalpy surface is explored by performing consecutive short molecular dynamics escape steps followed by local geometry relaxations taking into account both atomic and cell variables. The initial velocities for the molecular dynamics trajectories are chosen approximately along soft-mode directions, thus allowing efficient escapes from local minima and aiming toward low-energy structures. Revisiting already known structures is avoided by a feedback mechanism. The minima hopping method has already been used for structural prediction in a wide range of materials,[30−32] including the dependence on pressure,[33] with remarkable results.

Different approaches to global structural prediction have been used over the past years to obtain (meta-) stable structures for given stoichiometries and have enjoyed several remarkable successes.[34−36] Most often these methods aim at obtaining the crystal structure that minimizes the energy, but we should also mention a few attempts at optimizing other quantities. For example, Oganov and Lyakhov[37,38] and later Zhang et al.[39] used evolutionary algorithms to maximize the hardness, while Xiang et al.[40] optimized optical absorption.

For the determination of forces and energies within density functional theory (DFT) we used the code VASP[41,42] with the PAW data sets of version 5.2 (for compatibility with the Materials Project[9] and Open Quantum Materials databases[8]). We used a cutoff of 520 eV, and we selected our k-point grids to ensure an accuracy of 2 meV/atom in the total energy. All forces were converged to better than 0.005 eV/Å. To approximate the exchange-correlation functional of DFT we used the Perdew−Burke−Ernzerhof[43] (PBE) generalized gradient approximation. This setup was also used to evaluate the bulk and shear moduli and derived quantities. At the end of the simulation, all structures higher than 200 meV/atom from the ground state were disregarded. The remaining were reoptimized, and their properties were further calculated.

3. RESULTS

As a first showcase demonstration of our method, we decided to search for superhard materials. The hardness is a technologically important property that has been the subject of numerous studies over the past decades. We performed two independent GA runs with 15 generations each. This is a relatively small number for a stochastic method such as the GA, so we cannot expect that the simulations are completely converged. However, our data are already clearly sufficient to draw conclusions regarding the feasibility of our approach and to find several interesting materials. We used a population of 100 individuals, and we allowed all elements up to bismuth, but excluding the rare gases (which do not form hard compounds) and the lanthanides. We note that these choices were arbitrary and ultimately decided by efficiency reasons. The initial generation was chosen such that each individual contained four *random* atoms in the unit cell, making sure that each element appeared a minimum number of times in the initial generation. For each individual, the global structural prediction starting structure was also random, with the only constraint being that the atoms were separated by a certain minimum distance. A maximum of three different structural prediction runs was performed for each stoichiometry. Finally, the mating operations mixed the elements of both parents, while the mutations operated the alchemical transmutation of the elements. In total the structural prediction algorithm visited 121,000 minima for 1,500 compositions, of which 33,000 unique structures were further analyzed. All calculations were performed in around 1 million computer hours, a number relatively modest in comparison to the supercomputing resources currently available.

The calculation of the Vickers' hardness for the predicted structures is based on the model by Zhang et al.[39] This model extends the work of Šimůnek and Vackář,[44,45] and improves the

DOI: 10.1021/acs.jctc.5b00212
J. Chem. Theory Comput. 2015, 11, 3955−3960

earlier hardness models[46] based on bond strength by applying the Laplacian matrix[47] to account for highly anisotropic and molecular systems. In order to benchmark this model, we calculated the hardness for all materials contained in the open quantum materials database[8] (around 300,000 entries). It turns out that laminar systems are correctly described as having low hardness, but the model still fails for some molecular crystals that are incorrectly assigned large values for the hardness. This is, however, not a big problem as these false positive cases can be easily identified and discarded, as explained in the following.

In Table 1 we summarize Vickers' hardness, bulk modulus and shear modulus of all compounds identified in our GA simulations with a hardness larger than 40 GPa, i.e., that qualify as superhard materials. For the sake of comparison, we also include the distance to the convex hull of thermodynamic stability and the space group.

Table 1. Superhard Materials Found in Our GA Simulations[a]

system	spg	E_{hull}	hardness	bulk	shear
BC	5	413	123	304	270
C	227	136	97	444	526
CN_2	119	722	91	423	300
B	166	177	72	215	202
BC_3	25	308	71	359	321
BC_2	1	612	68	261	141
B_3C_2	1	452	63	162	82
C_2Si	166	497	54	268	273
HFe	216	164	52	226	95
HB	12	660	50	205	183
NMn	216	0	50	283	26
HCCo	8	625	50	92	23
HNi_2	123	40	49	220	85
HC_2	2	457	47	275	184
HBNi	1	401	46	123	12
H_3NO	8	314	45	38	10
HNi	44	14	45	191	23
CFe	216	479	44	260	55
C_2P	8	554	44	90	96
B2C	8	383	43	208	62
B_2C_3Si	1	345	42	204	162
NOs	119	410	42	300	86

[a]We show the space group of the structure (spg), the distance to the convex hull of stability (E_{hull}, meV), the Vickers' hardness (GPa), and the bulk and shear moduli (GPa).

Without great surprises, the hardest materials on this list are composed of B, C, and N. The only structure harder than diamond is a high-energy metastable low-symmetry structure of BC. In second place comes diamond, which also exhibits the highest bulk and shear moduli of all materials we looked at. For curiosity, we also found a carbon allotrope with a hardness higher than diamond, but too high in energy to enter our list, considering that we set a cutoff of 200 meV above the ground-state structure. Then comes CN_2 followed by a metastable allotrope of boron (that has a larger hardness than any other known boron structure present in the open quantum materials database[8]) and by several boron carbides. All of these materials are characterized by short and strong covalent bonds. Further down on the list we can also find a few transition metal nitrides (MnN, OsN) and several materials containing hydrogen.

We also obtained a few false positives, such as HCCo, H_3NO, or C_2P, as can be seen by their low bulk and shear moduli. This is due to the current limitations of the model used to estimate the hardness, but these cases are usually simple to spot and to filter out. For example, H_3NO turns out to be a molecular crystal that the model failed to recognize as such. We should also note that most of the materials present in the table are not thermodynamically stable, as can be seen by the finite value of E_{hull}; i.e., they can a priori decompose to other compounds or to more stable phases of the same compound. However, superhard materials are usually quite compact and are normally stabilized by pressure. It is therefore not unthinkable that some of these phases can be produced by a high-pressure synthesis procedure, analogously to diamond (the second entry of the list).

The evolution of the hardness during our GA simulations is shown in Figure 1 for our two independent runs. The lines are a guide to the eye and represent the maximum (top line), average (middle line), and minimum (bottom line) hardness in a given generation. Some of the most relevant compounds that appeared during the evolution are also indicated in the figure. The average hardness increases almost monotonically, as the GA narrows the search space. Moreover, diamond (labeled "C" in the plot) appears already in the ninth generation of run I and in the fifth generation of run II. This is somewhat surprising as,

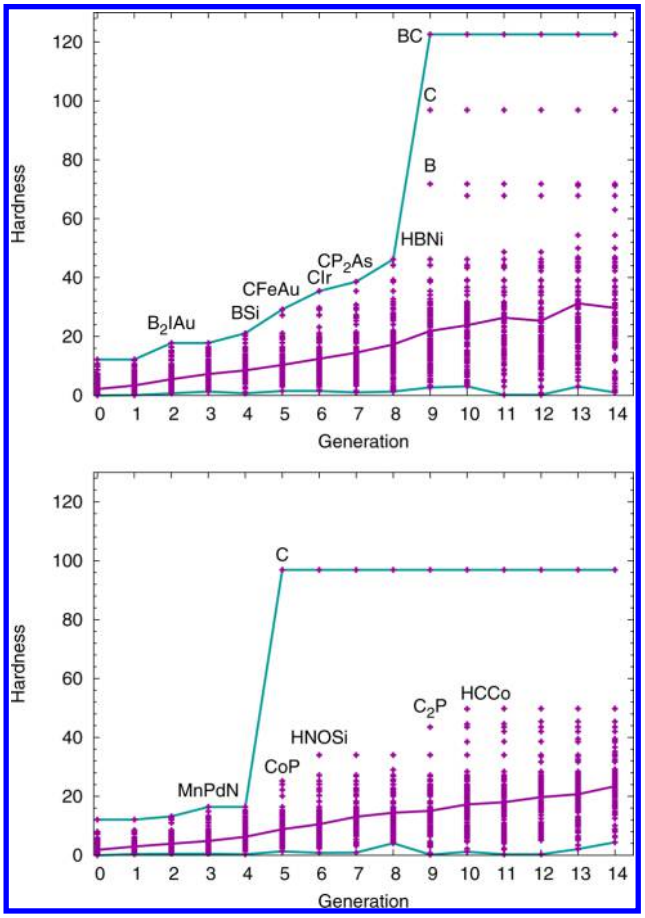

Figure 1. Evolution of the maximum (top line), minimum (bottom line), and average (middle line) hardness as a function of the generation for the two runs described in the text. Each point corresponds to the maximum hardness of a specific composition. Some relevant compounds are also indicated.

DOI: 10.1021/acs.jctc.5b00212
J. Chem. Theory Comput. 2015, 11, 3955−3960

up to that point, only a few hundred materials had been tested, which should be compared to the size of the search space that contains more than *61 million* possible compositions. We finally note that the path from the random initial materials to diamond goes through very unstable structures, obviously not present in any experimental database. This is certainly a key for the efficiency of the method.

To understand how the method works, we can analyze in Figure 2 the histogram measuring the frequency with which

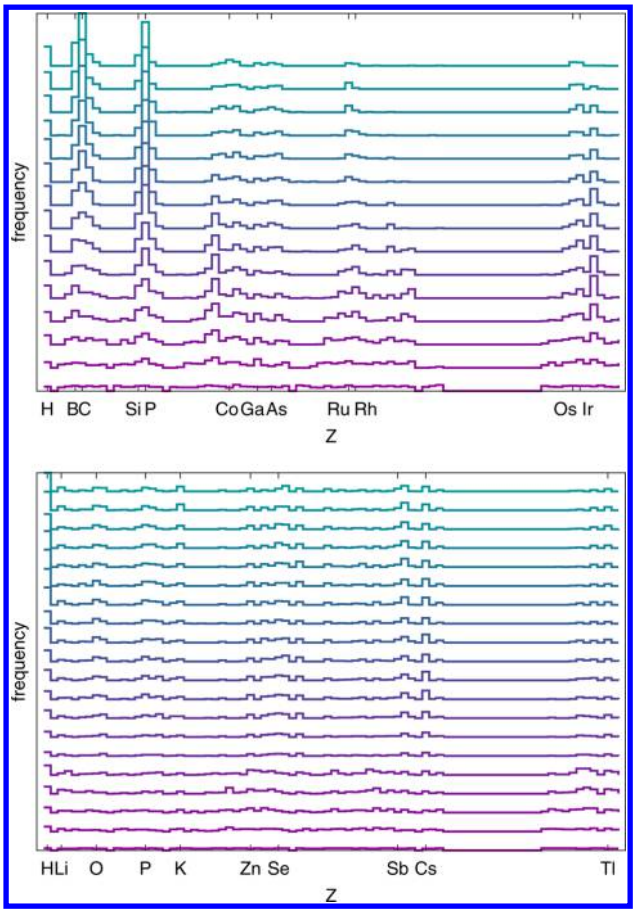

Figure 2. Frequency of the elements present in each generation of GA runs. Upper panel: Maximization of the hardness. The bottom line corresponds to generation 0, and the top line, to generation 14. Lower panel: Maximization of the band gap and minimization of the hole effective mass. The bottom line corresponds to generation 0, and the top line, to generation 19.

each element appears in a given generation. For the time being, we focus on the upper panel, which refers to the case of the optimization of the hardness. For the initial generation (the bottom line) there is an essentially uniform distribution (the zeros correspond to the elements explicitly excluded). This simply reflects our random choice of compositions for the starting generation. However, rather quickly several elements are excluded from our population, while others increase substantially their frequency. Among the latter there are H, B, C, N, Si, and P, etc., elements known to yield hard materials due to their short covalent bonds,[48−51] and several transition metals such as Ru, Rh, Os, and Ir, etc., that form hard nitrides, borides, and carbides, etc.[52,53] In a way, the GA is re-discovering, in a fully automatic and ab initio way, some of the basic intuition concerning hardness that physicists and metallurgists developed over the centuries.

As a more complicated test, we decided then to look at transparent conductors. In a recent work, Hautier et al. conducted a high-throughput computational search on thousands of binary and ternary oxides and they identified several highly promising compounds.[15] Two key properties to optimize are the electronic band gap, which has to be sufficiently large to ensure transparency, and the hole effective mass, which needs to be small to allow for mobile carriers. Such requirements can be easily accommodated in our framework using a multiobjective optimization algorithm.

We performed 20 generations with a setup similar to the one for the runs for the hardness. In total we investigated 1,100 compositions, leading to 72,000 minima, of which 19,000 were further analyzed.

Gaps and hole effective masses (m_h^*) were calculated using the PYMATGEN[54] and BoltzTrap[55] software packages. We used the PBE[43] functional and the Heid−Scuseria−Ernzerhof[56,57] (HSE06) hybrid functional to calculate the band gaps. We note that the HSE06 functional is a screened hybrid that gives very good values for the electronic gap of small and medium gap semiconductors. In particular, the HSE06 estimate is much better than the PBE one, which has the tendency to underestimate substantially the electronic gaps. The dispersion of the bands is however much less sensitive to the choice of the exchange-correlation functional. For this reason, we extracted the average hole effective mass from PBE Kohn−Sham band structures, following the same approach as that of ref 15. We calculated the averaged hole effective mass tensor for a carrier concentration of 10^{18} cm^{-3} and a temperature of 300 K. We then used the higher limit estimation (see Supporting Information of ref 15) of m_h^* as the input value for the GA. We note that only one structure per composition was used to evaluate m_h^*, which was not always the ground-state structure. Rather, we chose the structure with the largest gap within 50 meV from the ground state.

Our results are summarized in Figure 3 where we plot the average hole effective mass (in units of the electron mass) versus the electronic band gap (eV). Note that this latter quantity was calculated during the optimization runs using standard DFT, so its value is consistently underestimated.

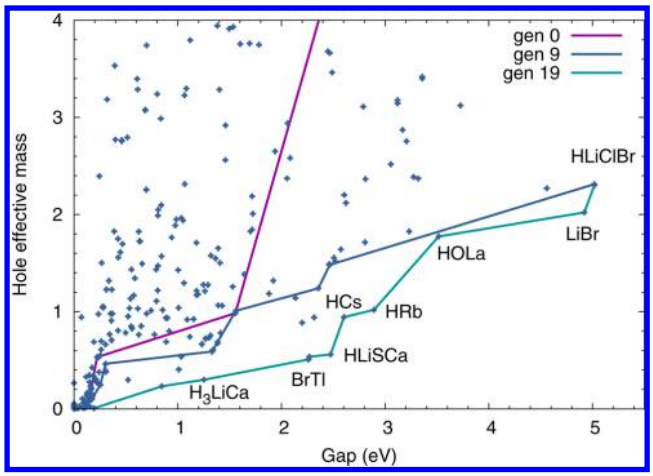

Figure 3. Average hole effective mass versus electronic band gap for all structures found in our run. The lines indicate the Pareto front for generations 0 (magenta), 9 (dark blue), and 19 (light blue).

DOI: 10.1021/acs.jctc.5b00212
J. Chem. Theory Comput. 2015, 11, 3955−3960

Again, our GA method works very efficiently. The Pareto front, i.e., the line connecting the structures with the best gap for each effective mass (or vice versa), is improved gradually from generation to generation. Several materials appear with large PBE gaps and small hole effective masses that are interesting candidates for transparent conduction.

Table 2 summarizes the results for all structures with a band gap larger than 1.0 eV and an average hole effective mass smaller than 1.5 electron masses. We list the crystallographic space group, the distance to the convex hull of thermodynamic stability (E_{hull}), the distance of the chosen structure to the lowest energy structure found for that composition (E_{GS}), the electronic band gap calculated with the PBE[43] functional and The Heid–Scuseria–Ernzerhof[56,57] (HSE06) hybrid functional, and the average hole effective mass (from PBE Kohn–Sham band structures).

Table 2. Best Candidate Transparent Conductive Materials Found during Our Simulations[a]

system	spg	E_{hull}	E_{GS}	E_{gap}^{PBE}	E_{gap}^{HSE}	m_h^*
PZnGeSeCs	1	57	11	1.06	1.41	1.29
ClKBrCdIn	8	79	38	1.25	1.69	1.28
HSSbTe	1	63	20	1.18	1.80	1.21
HSeCdTl	160	89	17	1.03	1.80	0.54
HSSb	8	173	22	1.01	1.80	1.04
HCaZnSb	8	0	1	1.01	1.91	0.41
HPCdTe	1	143	49	1.09	2.01	0.92
HSNbTe	1	0	0	1.27	2.03	0.72
OPTeTl	1	197	10	1.26	2.06	1.21
BeSZnTe	160	151	0	1.23	2.16	0.67
CaSeCdTe	156	124	3	1.41	2.24	0.78
SCa_2Te	166	50	0	1.38	2.37	0.69
FSiCaSeTeTl	1	225	48	1.15	2.37	0.92
BePSCs	1	272	0	1.41	2.41	1.50
SCaZn	156	496	1	1.30	2.45	0.73
H_2SbCs	1	42	0	1.56	2.46	0.98
HLiBrSbTe	8	119	6	1.53	2.46	1.26
OP	8	284	0	1.33	2.50	0.59
LiFCaSeTe	1	233	10	1.32	2.54	1.58
H_2STe	1	194	4	1.00	2.64	1.43
HSeCdAu	1	154	2	1.29	2.67	1.28
$H_2CaSbCs$	8	134	0	1.92	2.71	1.32
HSRh	1	148	0	1.36	2.79	1.55
CPTeCs	8	573	12	1.64	2.89	1.38
OZnGeSe	8	169	42	1.39	2.89	1.07
H_2NAu	1	233	0	1.12	2.97	0.74
MgTe	216	1	1	2.31	3.13	0.94
HLiCaTe	6	103	34	2.14	3.18	1.14
HRbTe	1	0	0	2.36	3.23	1.24
HSZnAu	1	163	0	1.88	3.27	1.19
HTeCs	8	0	0	2.46	3.33	1.49
HFCaTe	1	133	0	2.51	3.48	1.55
BrTl	6	1	29	2.26	3.71	0.51
H_3LiCa	221	28	0	1.25	3.95	0.30
HLiSCa	38	84	0	2.20	4.23	0.89
HCs	4	0	32	2.60	4.26	0.94
HRb	225	0	0	2.89	4.74	1.02

[a]We show the distance to the convex hull of stability (E_{hull}, meV), the distance to the ground-state (GS) structure found (E_{GS}, meV), the space group, the band gap from the PBE and the HSE06 exchange-correlation functionals (eV), and the average hole effective mass (m_h^* in electron masses).

The evolution of the composition as a function of the generation, for the simultaneous optimization of the band gap and the hole effective mass, can be found in the lower panel of Figure 2. In this case, the interpretation of the plot is more complicated than for the optimization of the hardness, as most of the successful structures are combinations of metallic elements with nonmetallic elements, and therefore it is less likely that an element disappears from the population during the evolution process.

It is however interesting to analyze in detail how the GA worked in this second case. Taking random compositions, the probability of finding semiconducting systems is fairly low. For example, our generation 0 contained only 13 semiconductors out of 100 individuals. The first step in the optimization was to find semiconductors. This could be achieved, e.g., by making molecular crystals formed mainly by nonmetals or by combining metallic and nonmetallic elements in the same structure. Since the first possibility yields very high effective masses, the final generation contains almost exclusively compounds of the latter kind. This again shows that the GA algorithm has re-discovered basic chemical rules without any human intervention.

4. CONCLUSIONS

In conclusion, we propose a new method to design on-the-fly new materials with tailored properties. Our first test maximizing the hardness or maximizing at the same time the electronic gap and the hole effective mass, was extremely successful, with several interesting, unknown materials stemming from the simulations. This shows that our method is not only perfectly feasible but also efficient with current computer resources. Of course any other property that can be calculated in a computer can be optimized, including the band gap, the Seebeck coefficient, the superconducting transition temperature, or even the price of the constituents. Finally, we stress that any pragmatic search for technologically relevant materials should also take into consideration the large databases of materials already existing (to generate, e.g., a good initial population). Conversely, the novel crystal structures encountered by our global prediction methods can also be incorporated into these databases.

We believe that our results are above all a proof of the incredible advances of ab initio calculations in the past decades and a prelude to what this field has to offer in the next ones.

AUTHOR INFORMATION

Corresponding Author

*E-mail: marques@tddft.org.

Funding

S.B. and M.A.L.M. acknowledge support from the French ANR (Grant ANR-12-BS04-0001-02). Financial support provided by the Swiss National Science Foundation is gratefully acknowledged.

Notes

The authors declare no competing financial interest.

ACKNOWLEDGMENTS

Computational resources were provided by GENCI (Project x2013096017) in France and the PRACE-3IP project (FP7 RI-

DOI: 10.1021/acs.jctc.5b00212
J. Chem. Theory Comput. 2015, 11, 3955–3960

312763) resource Archer based in Scotland at the University of Edinburgh.

REFERENCES

(1) von Lilienfeld, O. A. In *Many-Electron Approaches in Physics, Chemistry and Mathematics: A Multidisciplinary View*; Bach, V. , Delle Site, L., Eds.; Lecture Notes in Physics; Springer Verlag: Cham, Switzerland, 2014; DOI: 10.1007/978-3-319-06379-9.
(2) Curtarolo, S.; Hart, G. L. W.; Nardelli, M. B.; Mingo, N.; Sanvito, S.; Levy, O. *Nat. Mater.* **2013**, *12*, 191−201.
(3) Ceder, G. *MRS Bull.* **2010**, *35*, 693−701.
(4) Franceschetti, A.; Zunger, A. *Nature* **1999**, *402*, 60−63.
(5) Zhang, L.; d'Avezac, M.; Luo, J.-W.; Zunger, A. *Nano Lett.* **2012**, *12*, 984−991.
(6) d'Avezac, M.; Luo, J.-W.; Chanier, T.; Zunger, A. *Phys. Rev. Lett.* **2012**, *108*, 027401.
(7) Belsky, A.; Hellenbrandt, M.; Karen, V. L.; Luksch, P. *Acta Crystallogr., Sect. B: Struct. Sci.* **2002**, *58*, 364−369.
(8) Saal, J.; Kirklin, S.; Aykol, M.; Meredig, B.; Wolverton, C. *JOM* **2013**, *65*, 1501−1509.
(9) Jain, A.; Ong, S. P.; Hautier, G.; Chen, W.; Richards, W. D.; Dacek, S.; Cholia, S.; Gunter, D.; Skinner, D.; Ceder, G.; Persson, K. A. *APL Mater.* **2013**, *1*, 011002.
(10) Setyawan, W.; Curtarolo, S. *Comput. Mater. Sci.* **2010**, *49*, 299−312.
(11) Curtarolo, S.; Setyawan, W.; Wang, S.; Xue, J.; Yang, K.; Taylor, R. H.; Nelson, L. J.; Hart, G. L.; Sanvito, S.; Buongiorno-Nardelli, M.; Mingo, N.; Levy, O. *Comput. Mater. Sci.* **2012**, *58*, 227−235.
(12) Fiolhais, C., Nogueira, F., Marques, M., Eds. *A Primer in Density Functional Theory*; Springer: Berlin, 2003.
(13) Parr, R. G.; Yang, W. *Density-Functional Theory of Atoms and Molecules*; Oxford University Press: New York, NY, USA, 1994.
(14) Carrete, J.; Li, W.; Mingo, N.; Wang, S.; Curtarolo, S. *Phys. Rev. X* **2014**, *4*, 011019.
(15) Hautier, G.; Miglio, A.; Ceder, G.; Rignanese, G.-M.; Gonze, X. *Nat. Commun.* **2013**, *4*, No. 2292, DOI: 10.1038/ncomms3292.
(16) Pilania, G.; Wang, C.; Jiang, X.; Rajasekaran, S.; Ramprasad, R. *Sci. Rep.* **2013**, *3*, 2810.
(17) Fujimura, K.; Seko, A.; Koyama, Y.; Kuwabara, A.; Kishida, I.; Shitara, K.; Fisher, C. A. J.; Moriwake, H.; Tanaka, I. *Adv. Energy Mater.* **2013**, *3*, 980−985.
(18) von Lilienfeld, O. A.; Lins, R. D.; Rothlisberger, U. *Phys. Rev. Lett.* **2005**, *95*, 153002.
(19) Wang, M.; Hu, X.; Beratan, D. N.; Yang, W. *J. Am. Chem. Soc.* **2006**, *128*, 3228−3232.
(20) Keinan, S.; Hu, X.; Beratan, D. N.; Yang, W. J. *J. Phys. Chem. A* **2007**, *111*, 176−181.
(21) Anatole von Lilienfeld, O. *J. Chem. Phys.* **2009**, *131*, 164102.
(22) Balawender, R.; Welearegay, M. A.; Lesiuk, M.; De Proft, F.; Geerlings, P. *J. Chem. Theory Comput.* **2013**, *9*, 5327−5340.
(23) Lesiuk, M.; Balawender, R.; Zachara, J. *J. Chem. Phys.* **2012**, *136*, 034104.
(24) d'Avezac, M.; Zunger, A. *Phys. Rev. B: Condens. Matter Mater. Phys.* **2008**, *78*, 064102.
(25) Niu, H.; Chen, X.-Q.; Ren, W.; Zhu, Q.; Oganov, A. R.; Li, D.; Li, Y. *Phys. Chem. Chem. Phys.* **2014**, *16*, 15866−15873.
(26) Oganov, A. R., Ed. *Modern Methods of Crystal Structure Prediction*; Wiley-VCH: Berlin, 2010.
(27) Deb, K.; Pratap, A.; Agarwal, S.; Meyarivan, T. *IEEE Trans. Evol. Comput.* **2002**, *6*, 182.
(28) Amsler, M.; Goedecker, S. *J. Chem. Phys.* **2010**, *133*, 224104.
(29) Goedecker, S. *J. Chem. Phys.* **2004**, *120*, 9911−9917.
(30) Amsler, M.; Flores-Livas, J. A.; Lehtovaara, L.; Balima, F.; Ghasemi, S. A.; Machon, D.; Pailhès, S.; Willand, A.; Caliste, D.; Botti, S.; San Miguel, A.; Goedecker, S.; Marques, M. A. L. *Phys. Rev. Lett.* **2012**, *108*, 065501.
(31) Huan, T. D.; Amsler, M.; Marques, M. A. L.; Botti, S.; Willand, A.; Goedecker, S. *Phys. Rev. Lett.* **2013**, *110*, 135502.
(32) Amsler, M.; Botti, S.; Marques, M. A. L.; Goedecker, S. *Phys. Rev. Lett.* **2013**, *111*, 136101.
(33) Flores-Livas, J. A.; Amsler, M.; Lenosky, T. J.; Lehtovaara, L.; Botti, S.; Marques, M. A. L.; Goedecker, S. *Phys. Rev. Lett.* **2012**, *108*, 117004.
(34) Ma, Y.; Eremets, M.; Oganov, A. R.; Xie, Y.; Trojan, I.; Medvedev, S.; Lyakhov, A. O.; Valle, M.; Prakapenka, V. *Nature* **2009**, *458*, 182−185.
(35) Oganov, A. R.; Chen, J.; Gatti, C.; Ma, Y.; Ma, Y.; Glass, C. W.; Liu, Z.; Yu, T.; Kurakevych, O. O.; Solozhenko, V. L. *Nature* **2009**, *457*, 863−867.
(36) Gou, H.; Dubrovinskaia, N.; Bykova, E.; Tsirlin, A. A.; Kasinathan, D.; Schnelle, W.; Richter, A.; Merlini, M.; Hanfland, M.; Abakumov, A. M.; Batuk, D.; Van Tendeloo, G.; Nakajima, Y.; Kolmogorov, A. N.; Dubrovinsky, L. *Phys. Rev. Lett.* **2013**, *111*, 157002.
(37) Oganov, A.; Lyakhov, A. *J. Superhard Mater.* **2010**, *32*, 143−147.
(38) Lyakhov, A. O.; Oganov, A. R. *Phys. Rev. B: Condens. Matter Mater. Phys.* **2011**, *84*, 092103.
(39) Zhang, X.; Wang, Y.; Lv, J.; Zhu, C.; Li, Q.; Zhang, M.; Li, Q.; Ma, Y. *J. Chem. Phys.* **2013**, *138*, 114101.
(40) Xiang, H. J.; Huang, B.; Kan, E.; Wei, S.-H.; Gong, X. G. *Phys. Rev. Lett.* **2013**, *110*, 118702.
(41) Kresse, G.; Furthmüller, J. *Comput. Mater. Sci.* **1996**, *6*, 15−50.
(42) Kresse, G.; Furthmüller, J. *Phys. Rev. B: Condens. Matter Mater. Phys.* **1996**, *54*, 11169−11186.
(43) Perdew, J. P.; Burke, K.; Ernzerhof, M. *Phys. Rev. Lett.* **1996**, *77*, 3865−3868.
(44) Šimůnek, A.; Vackář, J. *Phys. Rev. Lett.* **2006**, *96*, 085501.
(45) Šimůnek, A. *Phys. Rev. B: Condens. Matter Mater. Phys.* **2007**, *75*, 172108.
(46) Gao, F.; Gao, L. *J. Superhard Mater.* **2010**, *32*, 148−166.
(47) Trinajstic, N.; Babic, D.; Nikolic, S.; Plavsic, D.; Amic, D.; Mihalic, Z. *J. Chem. Inf. Model.* **1994**, *34*, 368−376.
(48) Liu, A. Y.; Cohen, M. L. *Science* **1989**, *245*, 841−842.
(49) Vepřek, S. *J. Vac. Sci. Technol., A* **1999**, *17*, 2401−2420.
(50) Solozhenko, V. L.; Andrault, D.; Fiquet, G.; Mezouar, M.; Rubie, D. C. *Appl. Phys. Lett.* **2001**, *78*, 1385−1387.
(51) Solozhenko, V. L.; Gregoryanz, E. *Mater. Today* **2005**, *8*, 44−51.
(52) Friedrich, A.; Winkler, B.; Juarez-Arellano, E. A.; Bayarjargal, L. *Materials* **2011**, *4*, 1648−1692.
(53) Levine, J. B.; Tolbert, S. H.; Kaner, R. B. *Adv. Funct. Mater.* **2009**, *19*, 3519−3533.
(54) Ong, S. P.; Richards, W. D.; Jain, A.; Hautier, G.; Kocher, M.; Cholia, S.; Gunter, D.; Chevrier, V. L.; Persson, K. A.; Ceder, G. *Comput. Mater. Sci.* **2013**, *68*, 314−319.
(55) Madsen, G. K.; Singh, D. J. *Comput. Phys. Commun.* **2006**, *175*, 67−71.
(56) Heyd, J.; Scuseria, G. E.; Ernzerhof, M. *J. Chem. Phys.* **2003**, *118*, 8207.
(57) Heyd, J.; Scuseria, G. E.; Ernzerhof, M. *J. Chem. Phys.* **2006**, *124*, 219906.

DOI: 10.1021/acs.jctc.5b00212
J. Chem. Theory Comput. 2015, 11, 3955−3960